NASA Technical Memorandum 83034

Analysis of Combustion Spectra Containing Organ Pipe Tones by Cepstral Techniques

J. H. Miles and C. A. Wasserbauer
Lewis Research Center
Cleveland, Ohio

(NASA-TM-83034) ANALYSIS OF COMBUSTION SPECTRA CONTAINING ORGAN PIPE TONE BY CEPSTRAL TECHNIQUES (NASA) 29 p
HC A03/MF A01 CSCL 20A

N83-16153
Unclas
G3/71 02435

Prepared for the
One-hundred fourth Meeting of the Acoustical Society of America
Orlando, Florida, November 8-12, 1982

NASA

ANALYSIS OF COMBUSTION SPECTRA CONTAINING ORGAN PIPE TONES BY CEPSTRAL TECHNIQUES

by J. H. Miles and C. A. Wasserbauer

National Aeronautics and Space Administration

Lewis Research Center

Cleveland, Ohio

E-1472

ABSTRACT

Signal reinforcements and cancellations due to standing waves may distort constant bandwidth combustion spectra. Cepstral techniques previously applied to the ground-reflection echo problem are used to obtain smooth broad-band data and information on combustion noise propagation. Internal fluctuating pressure measurements made using a J47 combustor attached to a 6.44 m long duct are analyzed. Measurements made with Jet A and hydrogen fuels are compared. The acoustic power levels inferred from the measurements are presented for a range of low heat release rate operating conditions near atmospheric pressure. For these cases, the variation with operating condition of the overall acoustic broad-band power level for both hydrogen and Jet A fuels is consistent with previous results showing it was proportional to the square of the heat release rate. However, the overall acoustic broad-band power level generally is greater for hydrogen than for Jet A.

NOMENCLATURE

A	duct area ($0.0305 m^2$)
C(q)	cepstrum
c_o	speed of sound, m/s
c_p	specific heat at constant pressure, J/kg K
f	frequency, Hz
G(f)	rig system operation transfer function
g(t)	rig system operation function
L	duct length, m
ℓ	location of microphone relative to duct exit, m
(MW)	gas molecular weight
N(f)	combustion process spectrum
n(t)	combustion process function
P(f)	pressure power spectrum
p(t)	pressure function, Pa
p	duct ambient pressure, Pa
q	quefrency, s
$\mathcal{R}$	gas constant, J/kg K
T	temperature, K
t	time, s
W	air mass flow rate, kg/s
x	duct axial distance, m

Superscripts

(')	liftered function

INTRODUCTION

As part of a combustion noise research program, pressure measurements were made in a combustion rig at the NASA Lewis Research Center using both Jet A and hydrogen fuels. At all test conditions pressure spectra showed the presence of organ pipe tones due to longitudinal duct resonance modes in addition to the broad-band combustion noise spectra.

The presence of these organ pipe tones in the combustion spectra makes analyzing the experimental results difficult. For example, the spectra are not easily compared and the level of the integrated pressure may be determined by the tones. Moreover, these tones are rig dependent. Consequently, in comparing experimental data from different rigs the tones must be extracted so that the general trend of the broad-band spectrum can be determined. One approach to removing the tones is to hand draw smooth lines through the experimental spectra (Ref. 1). These hand smoothed spectra can be effectively used to understand the parametric behavior of combustion noise; however, this is a tedious approach in an age of high speed computers.

In this paper it is shown that cepstral techniques may be applied to obtain computer-smoothed combustion noise spectra. In addition, these techniques can be used to obtain information on sound propagation and reflection in the duct. This approach is possible because the measured signal can be considered to be composed of a combustion noise signal, reduced echoes of that signal due to reflections at the duct ends, and amplified echoes of that signal due to enhancement in the combustion zone. Each signal path is characterized by a different signal transfer function and a different signal arrival time.

The cepstral method is applied to both the hydrogen and Jet A combustion data. The major measured echo time delay is compared with the theoretical echo time delay over a range of operating conditions for hydrogen and Jet A fuels. The computer-smoothed combustion duct pressure spectra are then presented for typical operating conditions. Last, the acoustic power levels calculated from the smooth spectra for the two fuels are compared.

BACKGROUND

The power cepstrum was first described by Bogart, Healy and Tukey as a technique to determine echo arrrival times (Ref. 2). The power cepstrum of a function is a Fourier transform of the logarithm of the power spectrum of that function. The cepstrum literature and application procedures are reviewed by Childers, Skinner, and Kemerait in Ref. 3 and by Randall and Hee in Ref. 4. Cepstral techniques have been applied to the analysis of multicylinder engine exhaust noise (Ref. 5) and to the aeroacoustic ground reflection echo problem (Refs. 6 to 7).

In order to accurately describe operations in cepstral analysis which might be confused with similar operations in spectrum analysis Bogart et al. (Ref. 2) introduced a now classical set of terms which are anagrams of the equivalent frequency domain terms. The ones used herein are:

quefrency.....frequency

liftering.....filtering

rahmonic.....harmonic

Note that the unit of quefrency is time.

In this report, cepstrum analysis is briefly discussed before the experimental investigation is presented.

POWER CEPSTRUM ANALYSIS

In the simple model used to define the combustion rig signal analysis system the pressure signal measured in the duct, $p(t)$, due to the combustion process, $n(t)$, is modified by rig system operation, $g(t)$. The rig system operation function represents the results of the echoes from the combustion duct ends and the interaction of the echoes and the combustion source. The output of the system can be written as the following convolution integral:

$$p(t) = \int_{-\infty}^{t} n(\tau)\, g\,(t - \tau\,)\, d\tau \tag{1}$$

Taking the Fourier transform of Eq. (1) yields

$$F\left\{p(t)\right\} = N(f)G(f) \tag{2}$$

Where $N(f)$ is the combustion process spectrum and $G(f)$ is the rig system operation transfer function. The pressure spectrum is then given by

$$P(f) = \left|N(f)\right|^2 \left|G(f)\right|^2 \tag{3}$$

Taking the logarithm of Eq. (3) yields

$$\log\ P(f) = \log \left|N(f)\right|^2 + \log \left|G(f)\right|^2 \tag{4}$$

The inverse Fourier transform of Eq. (4) yields the power cepstrum

$$C(q) = F^{-1}\{\log P(f)\} = F^{-1}\{\log |N(f)|^2\} + F^{-1}\{\log |G(f)|^2\} \tag{5}$$

Provided the combustion source cepstrum and the rig system cepstrum occupy different quefrency ranges, the effects of the two systems are separable. Consequently, for this condition the individual contributions of each power cepstrum can be separated by liftering in the quefrency domain. Thus the smoothed cepstrum is

$$C'(q) = F^{-1}\{\log |N(f)|^2\} \tag{6}$$

The smoothed spectrum is obtained by Fourier transforming the smoothed cepstrum. Thus

$$\therefore \log P'(f) = F\{C'(q)\} \tag{7}$$

The procedure used to compute the Fourier transform is presented in Ref. 6.

EXPERIMENTAL INVESTIGATION

The combustion process in a turbofan engine is a source of far-field noise. At the NASA Lewis Research Center an extensive program was conducted to determine the source and characteristics of combustion noise and its

propagation using aircraft gas turbine engines, combustor test facilities and ducted combustion rigs (Refs. 8 to 14). Jet A fuel was used in these tests. In order to determine if using a gaseous fuel changed the combustion noise source or combustion noise propagation, a program was initiated using gaseous hydrogen and Jet A for the fuels in a ducted combustion rig.

The experimental apparatus is shown schematically in Fig. 1. The combustor rig is shown in Fig. 1a. The combustor section consists of a 0.2m diameter by 0.77m long J-47 burner can placed concentrically in a 0.3m diameter by 0.77m long flow duct. The combustor section is followed by a 0.203m diameter by 6.44m long flow duct. The cut-off frequency of the long duct is above 1500 Hz. The Jet A and hydrogen fuel injection schematic is shown in Fig. 1b. Note, that the hydrogen is injected at the same point in the J-47 burner can as the Jet A.

The dynamic pressure measurements were made simultaneously in the duct at the four locations shown in Fig. 1 (one just upstream of the combustor and three in the long duct at 0.3m, 0.7m, and 6.14m from the long duct inlet) and at 3 far-field microphone locations (30, 90, and 120 degrees). Typical results from the microphone in the duct at 6.14 m only are presented in this paper.

The internal pressure transducers used were conventional 0.635m microphones with pressure response cartridges. In order to avoid direct exposure of the microphones to the combustion gases, they were mounted outside the ducted combustion rig and the fluctuating pressure in the rig was transmitted to the transducers by means of a "semi-infinite" acoustic wave guide. Details on these probes are given in Ref. 8.

The signals from the four internal probes and three far-field microphones were FM recorded on magnetic tape in 2 minute record lengths for

later processing. The internal probes and far-field microphones were calibrated with a piston phone prior to each day's running. The constant bandwidth spectra given in this paper were obtained by off-line processing of the taped data on a two-channel fast Fourier transform digital signal processor with a built-in a-d converter and 120dB/octave anti-aliasing filters. The processor was capable of direct computation of up to 4096 ensemble averages of a 1024 point forward or inverse Fourier transform to yield either time-domain or frequency domain information.

All tests were conducted in an outdoor acoustic arena. The facility is shown in Fig. 2.

The results discussed here were obtained at nominal mass flows of 0.6, 1.3, and 2.1 kg/s and at nominal temperatures of 760 K, 920 K, and 1090 K for hydrogen and Jet. A. The operating conditions are summarized in Tables I - III.

RESULTS

Measured Spectra

Typical logarithmic pressure spectra measured in the combustion duct near the exit are shown in Figs. 3 and 4 for Jet A and hydrogen fuel, respectively. The spectrum for Jet A was measured at a combustor exit temperature of 1093 K at an air mass flowrate of 0.55 kg/s. The spectrum for hydrogen was measured at a combustor exit temperature of 1036 K at an air mass flowrate of 0.62 kg/s. Note that the ripples in the hydrogen spectra have a much larger amplitude than those in the Jet A spectrum. Similar variations in spectra were observed at the other test conditions covered in the study.

In each case the spectrum consists of a sequence of harmonic peaks and dips superimposed on an underlying broad-band structure. The spectra have a rippled appearance. The peaks of the ripples occur approximately at frequencies $f_n = (n+1/2)c/2L$. Moreover, the peaks show a regular variation of amplitude with frequency. The pattern which is most common is as follows: peaks are small at lower frequencies; at intermediate frequencies an amplitude maximum is reached; finally, at high frequencies the ripple amplitude is small again.

Cepstra

Cepstra calculated from the spectra shown in Figs. 3 and 4 are shown in Figs. 5 and 6. All the cepstra examined for a range of test conditions have a fundamental pattern consisting of a large narrow negative spike near a quefrency of 0.03s with two adjacent positive spikes located on either side (see Fig. 5). The large excursion near 0.03s corresponds to the reciprocal of the spacing between the harmonics of 30 Hz shown in Figs. 3 and 4. Also shown in Fig. 5 is a set of smaller excursions near 0.06s which are first rahmonics. This pattern is related to the way a plane wave propagates in the duct. The cepstra represent the interaction of the following elements: amplification in the combustion region, wave reflection at inlet and exit of the combustion system, the position of the microphone, the length of the duct, and the flow and sound velocities. A mathematical model of the system should yield not only autoand cross-spectra but also the cepstra. Such a model should provide a complete explanation of the fundamental pattern.

The large narrow negative spike occurs in the fundamental pattern at the time (quefrency) it takes a signal to travel up and down the duct

$$q_0 = \int_0^L \frac{dx}{c(x)+v(x)} + \int_0^L \frac{dx}{c(x)-v(x)} = \frac{2L}{\bar{c}(x)\Big|_{x=L}} \tag{8}$$

Furthermore, adjacent to this negative spike are two positive spikes at times (quefrencies)

$$q_1 = \frac{2\,(L-\ell)}{\bar{c}(x)\Big|_{x\,=\,L}} \tag{9}$$

and

$$q_1 = \frac{2(L-\ell)}{\bar{d}(x)\Big|_{x\,=\,L}} \tag{10}$$

where ℓ is the distance between the infinite tube microphone and the duct exit.

The spike at quefrency q_1 is narrow while the spike at quefrency q_2 is broad. Also, each cepstrum has an inverse of this fundamental pattern at the second rahmonic quefrencies $2q_0$, $2q_1$, and $2q_2$. Moreover, in some cases the fundamental pattern is repeated at $3q_0$, $3q_1$, and $3q_2$.

The following simple analysis is used to correlate the quefrency of the major negative peak in the cepstra with the airflow rate, duct inlet temperature and duct exit temperature. Because the temperature distribution was not measured, it is assumed, for convenience, to be exponential. The duct temperature variation with position is assumed to be

$$T(x) = T(x)\Big|_{x = 1.07m} e^{-\alpha(x-1.07)}_{0<x<7.21m} \tag{11}$$

where

$$\alpha = -\left|n\left\{\frac{T(x)\Big|_{x = 1.07m}}{T(x)\Big|_{x = 6.91m}}\right\}\right| 5.84 \tag{12}$$

The isentropic speed of sound is given by

$$c_o(x) = 19.61 \sqrt{T(x)} \tag{13}$$

where the gas specific heat ratio used is 1.4 and is assumed to be independent of x. The flow velocity is assumed to be given by

$$v(x) = \frac{W \mathscr{R} T(x)}{A \; p_o (MW)} \tag{14}$$

where the gas molecular weight is also assumed to be independent of x.

Substituting Eqs. (11) to (14) into Eq. (8), using the measured temperature and air flows shown in Table III, and numerically integrating yields the theoretical echo travel time, $(q_o)_T$, shown in Table III. The measured echo travel times corresponding to the quefrency of the major negative spike, $(q_o)_M$, are also shown in Table III. The variance of the theoretical echo travel time from the measured echo travel times was about 20 $(ms)^2$. However, the differences between the measured and theoretical values showed systematic trends which could be empirically correlated with mass flow and temperature using

$$(q_o)_E = \varepsilon(q_o)_T \, W^{\beta} \, T^{\delta}(x) \Big|_{x = 1.07m} \tag{15}$$

and the following exponents

$$\varepsilon = 0.505$$

$$\beta = -4.53 \times 10^{-3}$$

$$\delta = 0.106$$

The variance with this equation was reduced to about 1 $(ms)^2$. The magnitude of the exponents indicates that a small correction in the temperature distribution function might improve the model while changes related to the mass flow would make it less accurate. These results show that the cepstrum procedure is useful in the study of models for sound propagation in the combustion duct.

Furthermore, these results indicate that the sound propagated at the normal isentropic speed in the hydrogen and the Jet A fueled tests conducted using this facility. However, the echo time delay measurement does not provide information on the variation of the sound speed with frequency. An analysis of cross spectra, which is beyond the scope of this paper, would provide more definitive information on the variation of the speed of sound with frequency.

The fundamental cepstrum pattern (large narrow negative spike with adjacent positive spikes) appears since part of the measured signal consists of three signals which can be considered to have started at the microphone and traveled distances $2(L - \ell)$, $2L$ and $2(L + \ell)$ before returning to the microphone. Each of these signals underwent different reflections

along the path it traveled. The inlet of the combustion system acts like a closed tube so that the reflection factor at the inlet is $R = 1$. The exit of the duct is assumed to have a $R = 1$ reflection factor. The spike at q is negative because a signal traveling a distance $2L$ then has a $R = 1$ and a $R = -1$ reflection. Consequently, after the echo delay time the direct signal and the echo are 180 degrees out of phase and they will combine destructively. However, a signal traveling a distance $2(L - \ell)$ has only an $R = 1$ reflection. Thus, the echo undergoes no phase shift. While a signal traveling a distance $2(L + \ell)$ has an $R = 1$ reflection and two $R = -1$ reflections and undergoes a 360 degree phase shift. For these cases after the corresponding echo delay times the direct signal and a copy of the direct signal then will combine constructively.

Note that the signal that travels a distance $2(L + \ell)$ and had an $R = 1$ reflection and two $R = -1$ reflections is the one responsible for the higher quefrency positive broad spike in the fundamental pattern. Therefore, for this signal path more dispersion in travel times is present than along the signal paths which have one or no reflections from the duct exit.

Most of the hydrogen cepstra show many additional spikes in addition to the fundamental pattern (Fig. 6). However, at the higher air flow rates the hydrogen cepstra resemble the Jet A cepstra and only the fundamental pattern is observed.

Smoothed Spectra

Smoothed spectra produced by liftering and inverse Fourier transforming the cepstra presented in Figs. 5 and 6 are shown in Figs. 7 and 8. For Jet A combustion with a combustor exit temperature of 1093 K at a mass flow rate

of 0.55 kg/s the duct exit smoothed spectrum is shown in Fig. 7. The spectrum has a flat appearance. The smoothed hydrogen spectrum measured at a combustor exit temperature of 1036 K at an air mass flow rate of 0.62 kg/s is presented in Fig. 8. The hydrogen spectrum has a peaked appearance.

In order to obtain these smooth spectra, the following liftering procedure was used to preserve the broad-band spectral shape while removing most of the harmonic ripple in the measured spectrum. Since most of the broad bank spectral information is present in the cepstra at quefrencies below 0.0046 s, at quefrencies greater than 0.0046 s excursions greater than +10 and -10 were set to zero. Then new values were obtained at quefrencies which are zero by linear interpolation.

This liftering procedure is somewhat arbitrary. For example, it is possible to remove excursions greater than +5 and -5 or +1 and -1. Somewhat smoother spectra are obtained by removing excursions greater than +5 and -5. However, removing excursions greater than +1 and -1 may produce smooth but distorted spectra if the corresponding cepstrum has many large rahmonics.

The degree of smoothness and the acceptability of the spectrum after liftering are subjective decisions. However, for a wide range of choices the resulting overall broad-band power levels after lifterinng are in good agreement. For a typical spectrum having tones where the maximum level change between a cancellation and a reinforcement is 10 dB, the resulting overall power level before smoothing was 142.02 dB. Liftering by removing excursions of +10 and -10, +5 and -5, and +1 and -1 in the cepstrum yields overall broad-band power levels of 140.72, 140.60, and 140.57, respectively. As another example, for a typical spectrum having tones where the maximum level change between a cancellation and a reinforcement is 30 dB, the resulting overall power level was 146.92 dB. Liftering by removing

excursions of +10 and -10, +5 and -5, and +1 and -1 in the cepstrum yields overall broad-band power levels of 133.48, 133.53, and 134 db, respectively. Consequently, for the cases studied the scatter in the overall broad-band power levels obtained from smoothed spectra by using any of these sets of limiting values in the liftering procedure is less than 1 dB.

The significant differences between the Jet A and hydrogen spectra are not due to propagation since (1) the fundamental cepstrum pattern (large narrow negative spike with adjacent positive spikes) occurs in both sets of data and (2) the sound propagates at the normal isentropic speed in both Jet A and hydrogen. Consequently, in order to understand why the measured variation of the spectra with operating condition occurs, the combustion process and the combustion noise must be studied simultaneously.

Correlation with Heat Release Rate

The overall acoustic broad-band power levels (OAPWL) were obtained from the smoothed duct spectra. In calculating the overall pressure levels the fluctuating pressures are assumed to be acoustic. The sound power level (re. 10^{-13} watts) is calculated assuming plane wave propagation of the pressure perturbation. Various methods for relating the total pressure level to the steady state operating conditions have been described in Refs. 15 and 16.

The correlation of overall acoustic broad-band power level and heat release rate squared is shown in Fig. 19 for Jet A and hydrogen where $Q = W\, c_p\, \Delta T$. It is apparent that significant scatter exists in the acoustic power level data. However, for this system operating at atmospheric pressure and low heat release rates, the overall power level dependence on the square of the heat release rate is consistent with previ-

ous data. For example, this same dependence was also found in a study of core noise turbofan data from can combustors (Ref. 16) and annular combustors (Ref. 9) for the low heat release rates. Furthermore, the hydrogen overall acoustic broad-band power level for low heat release rates is about 3 dB greater than the Jet A overall acoustic broad-band power level at the same heat release rate.

CONCLUSIONS

Based on the application of cepstral techniques to the study of the pressure auto spectra measured near the exit of a long duct connected to a J-47 combustor using both hydrogen and Jet A fuels it is concluded that:

(1) The cepstra have a fundamental pattern (large narrow negative spike with adjacent positive spikes) due to signal propagation along three different paths.

(2) The fundamental pattern in the cepstra can be used to extract information on sound propagation in the duct.

(3) The quefrency of the large negative spike in the measured cepstra is consistent with the isentropic propagation of sound in both the Hydrogen and Jet A.

(4) Organ pipe tones can be removed from measured spectra by a liftering technique.

(5) The scatter in the overall broad-band power levels obtained from spectra smoothed by using three liftering techniques is less than 1 dB.

(6) Differences between the Jet A and hydrogen spectra for the same test condition are due to the combustion source region and not propagation effects.

(7) The variation with operating condition of the overall acoustic broad-band power level for tests using both hydrogen and Jet A is consistent with previous data that found it was proportional to the square of the heat release.

(8) The hydrogen overall acoustic broad-band power level for low heat release rates is greater than the Jet A overall acoustic broad-band power level at the same heat release rate.

REFERENCES

1. Belur N. Shivashankara and Robert W. Crouch, "Combustion noise characteristics of a can type combustor," AIAA paper No. 76-578 (July 1976).
2. B. P. Bogert, M. J. Healy, and J. W. Tukey, "The quefrency alanysis of time series for echoes: cepstrum, pseudo-autocovariance, cross-cepstrum, and saphe cracking," in Time Series Analysis, M. Rosenblatt, Ed. New York: Wiley, 1963, Chap. 15, pp. 209-243.
3. Donald G. Childers, David P. Skinner, and Robert C. Kemerait, "The cepstrum; guide to processing,: Proc. IEEE, 65, 1428-1443 (1977).
4. R. B. Randall and Jens Hees, "Cepstrum analysis," Bruel & Kjaer Technical Review, 3, 3-40 (1981).
5. K. Bright and D. W. Thomas, "Effect of manifold design and firing order on the short term spectrum," J. Sound and Vib., 48, 393-403 (1976).
6. J. H. Miles, G. H. Stevens, and G. G. Leininger, "Application of cepstral techniques to ground-reflection effects in measured acoustic spectra," J. Acoust. Soc. Am. 61, 35-38 (1977).
7. A. A. Syed, J. D. Brown, M. J. Oliver and S. A. Hills, "The cepstrum; a viable method for the removal of ground reflections,: J. Sound Vib., 71, 299-313 (1980).

8. Allen Karchmer and Meyer Reshotko, "Core noise source diagnostics on a turbofan engine using correlation and coherence techniques," 92nd meeting of the Acoustical Society of America, Nov. 16-19, San Diego, California, (1975); also NASA TM X-73535 (1976).

9. Meyer Reshotko and Allen Karchmer, "Core noise measurements from a small, general aviation turbofan engine," 100th meeting of the Acoustical Society of America, Nov. 17-21, Los Angeles, California (1980); also NASA TM-81610 (Nov. 1980).

10. Allen Karchmer, "Conditioned pressure spectra and coherence measurements in the core of a turbofan engine," AIAA Paper No. 81-2052 (Oct. 1981); also NASA TM-82688 (1981).

11. Eugene A. Krejsa, "New technique for the direct measurement of core noise from aircraft engines," AIAA Paper No. 81-1587 (Oct. 1981).

12. J. H. Miles, "Pressure transfer function of a JT15D nozzle due to acoustic and convected entropy fluctuations," 103rd meeting of the Acoustical Society of America, Apr. 26-30, Chicago, Illinois (1982); also NASA TM 82842 (1982).

13. Craig A. Wilson and James M. O'Connell, "YF 102 in-duct combustor noise measurements with a turbine nozzle," NASA CR-16552 (Sept. 1981).

14. J. H. Miles and D. D. Raftopoulos, "Spectral structure of pressure measurements made in a combustion duct," J. Acoust. Soc. Am., 68, 1711-1722 (1980).

15. Ronald G. Huff, Bruce J. Clark, and Robert G. Dorsch, "Interim prediction method for low frequency core engine noise," NASA TM X-71627 (Nov. 1974).

16. U. H. von Glahn, "Correlation of combustor acoustic power levels inferred from internal fluctuating pressure measurements," NASA TM-78986 (1978).

TABLE I. - JET A TEST CONDITIONS

Test point	W, kg/s	COMBUSTOR		Q, MW	P, N/m^2	OASPL, dB
		T_{AIR}, °K	T_{EXIT}, °K			
61	0.58	278	761	0.31	1.01	124.80
59	.57	279	916	.42	1.02	125.50
37	.55	278	1093	.54	1.01	126.40
44	1.24	278	759	.66	1.08	132.90
46	1.27	278	924	.95	1.09	134.40
48	1.26	279	1090	1.23	1.10	136.70
54	2.11	278	756	1.12	1.25	141.60
56	2.12	279	925	1.58	1.27	143.10
58	2.13	279	1092	2.07	1.28	143.10

TABLE II. - HYDROGEN TEST CONDITIONS

Test point	W, kg/s	COMBUSTOR		Q, MW	P, $N/M^2 x 10^5$	PWL, dB
		T_{AIR}, °K	T_{EXIT}, °K			
30	0.57	276	755	0.30	1.01	128.70
8	.63	276	923	.48	.990	133.50
9	.62	276	1036	.57	.991	136.40
3	1.29	276	755	.69	1.00	139.50
1	1.26	276	924	.96	1.00	140.03
6	1.30	277	1092	1.28	1.01	138.30
22	2.14	276	756	1.15	1.04	138.60
24	2.15	277	922	1.62	1.04	141.10
21	2.13	276	1098	2.12	1.06	142.90

TABLE III. – RESULTS OF ECHO TRAVEL TIME ANALYSIS.

Test point	Duct temperature		Pressure, p, $Pax10^{-5}$	Air flow, W, kg/s	Echo travel times		
	Inlet	Exit			Measured	Theoretical	Empirical
	$T(x)\|_{x=1.07m}$ °K	$T(x)\|_{x=6.91m}$ °K			$(q_o)_M$, s	$(q_o)_T$, s	$(q_o)_E = \varepsilon(q_o)_T W^{\beta} T_{IN}^{\delta}(1.07)$, s
1	924.0	679.0	1.01	1.26	0.02783	0.02687	0.02790
3	755.0	599.0	1.01	1.29	.02930	.02906	.02953
6	1092.0	758.0	1.02	1.30	.02637	.02522	.02665
8	923.0	711.0	.992	.63	.02686	.02601	.02708
9	1036.0	783.0	.992	.62	.02588	.02468	.02502
21	1099.0	745.0	1.09	2.13	.02783	.02655	.02801
22	756.0	562.0	1.06	2.14	.03125	.03066	.03109
24	922.0	657.0	1.07	2.15	.02906	.02840	.02941
30	755.0	568.0	.994	.57	.02930	.02885	.02943
37	1093.0	819.0	.992	.55	.02539	.02404	.02551
44	759.0	585.0	1.02	1.24	.02979	.02912	.02961
46	924.0	684.0	1.02	1.27	.02783	.02682	.02784
48	1090.0	797.0	1.03	1.26	.02637	.02487	.02627
54	756.0	575.0	1.06	2.11	.03125	.03045	.03088
56	924.0	667.0	1.08	2.12	.02939	.02819	.02920
58	1092.0	764.0	1.09	2.13	.02783	.02645	.02788
59	915.0	694.0	.995	.57	.02734	.02618	.02725
61	761.0	583.0	.995	.58	.02979	.02861	.02921
						$\delta^2 = 20(ms)^2$ (M_T)	$\delta^2 = 1(ms)^2$ $\varepsilon = 0.505$ $\beta = -4.53x10^{-3}$ $\delta = 0.106$ (M_E)

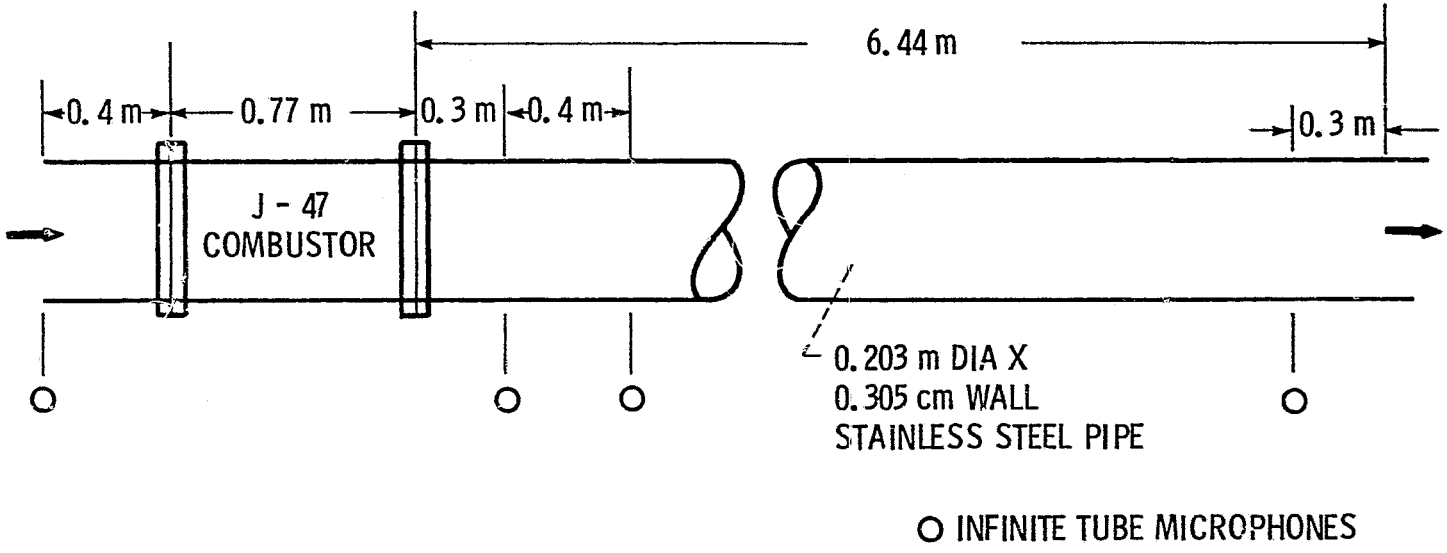

(a) Rig schematic.

Figure 1. - Schematic of ducted combustion system rig.

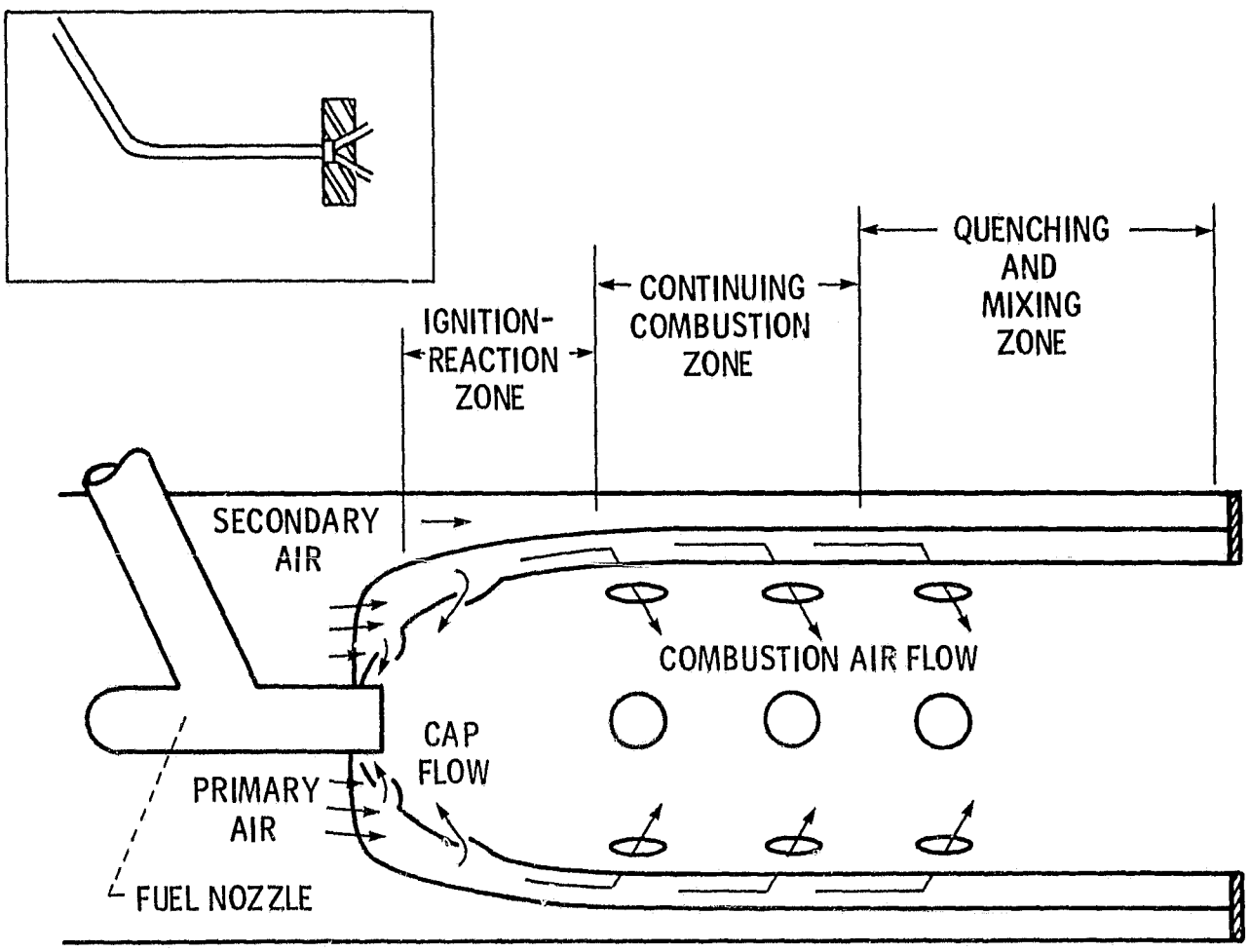

(b) Injection scheme.

Figure 1. - Concluded.

Figure 2. - NASA Lewis combustion acoustics facility.

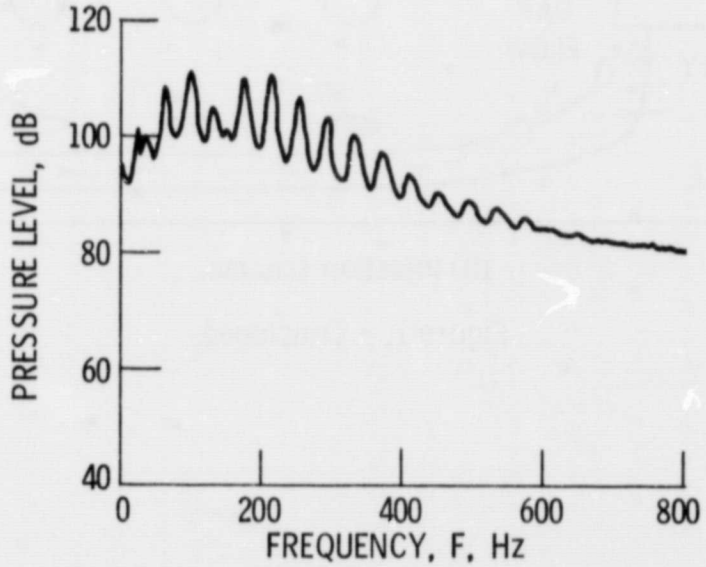

Figure 3. - Duct exit spectra (bandwidth = 2 Hz) for Jet A combustion at a combustor exit temperature of 1093 K at a mass flow of 0.55 kg/s.

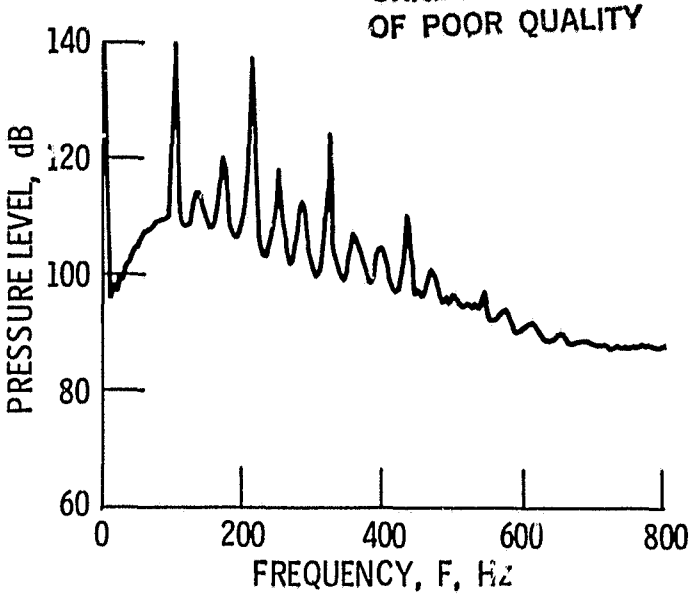

Figure 4. - Duct exit spectra (bandwidth = 2 Hz) for hydrogen combustion with a combustor exit temperature of 1036 K at a mass flow rate of 0.62 kg/s.

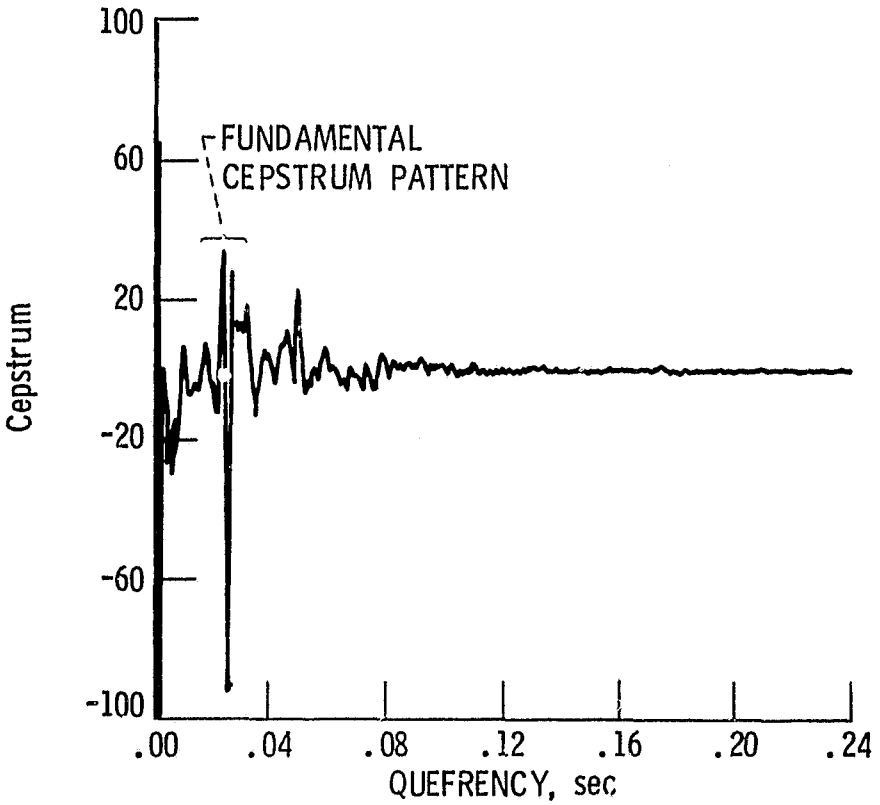

Figure 5. - Duct exit cepstra for Jet A combustion with a combustor exit temperature of 1093 K at a mass flow rate of 0.55 kg/s.

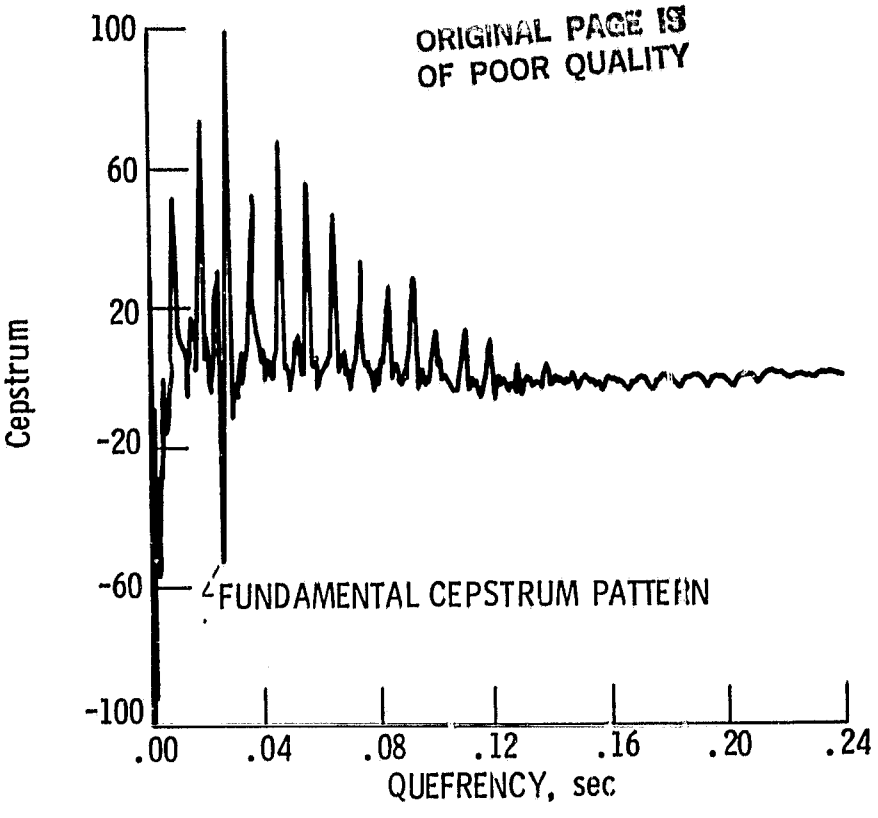

Figure 6. - Duct exit cepstra for hydrogen combustion with a combustor exit temperature of 1036 K at a mass flow rate of 0.62 kg/s.

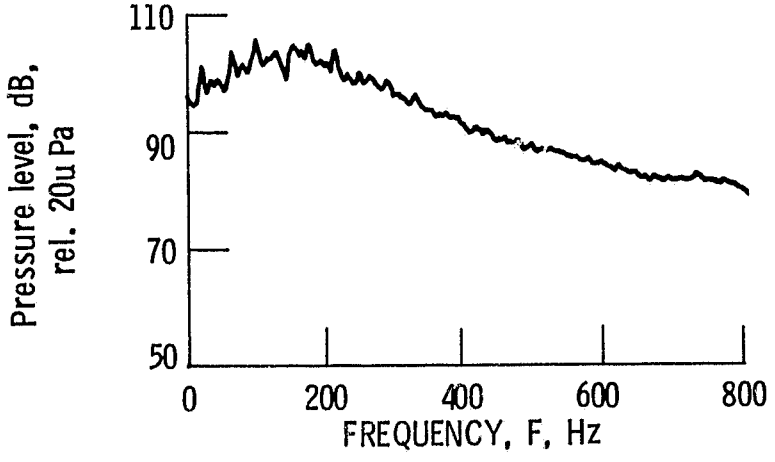

Figure 7. - Smoothed duct exit spectrum for Jet A combustion with a combustor exit temperature of 1093 K at a mass flow rate of 0.55 kg/s.

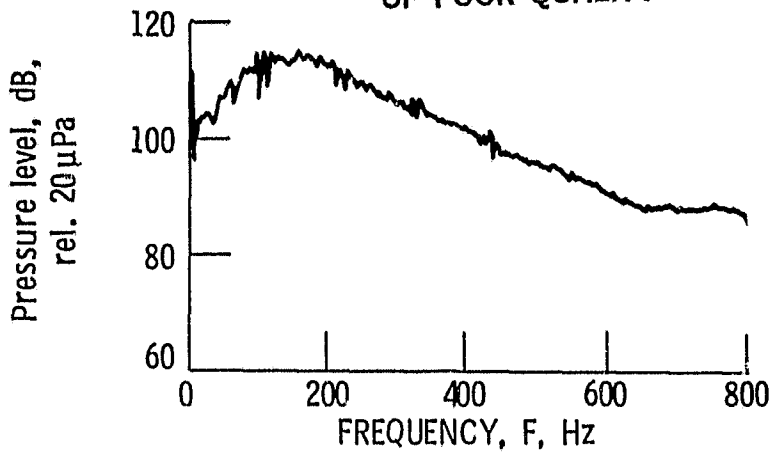

Figure 8. - Smoothed duct exit spectra for hydrogen combustion with a combustor exit temperature of 1036 K at a mass flow rate of 0.62 kg/s.

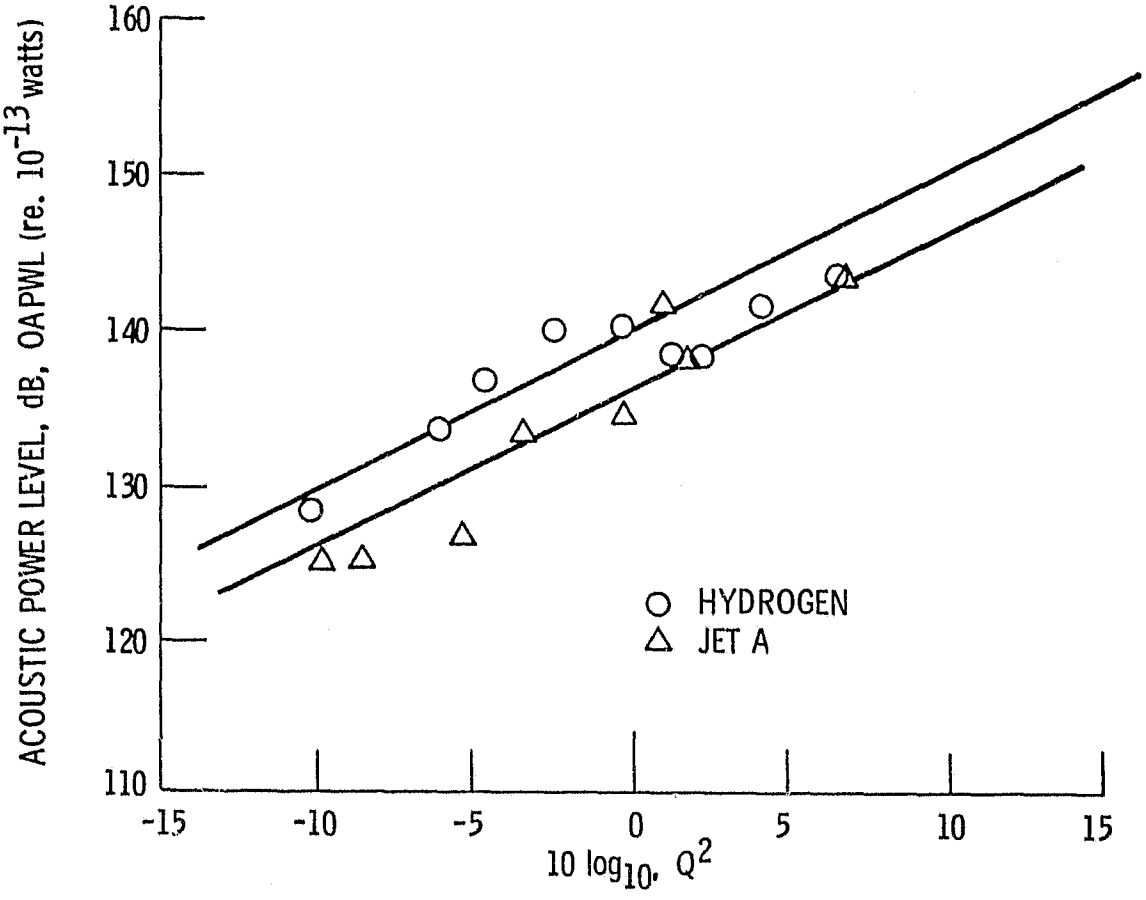

Figure 9. - Correlation of combustion noise and square of heat release rate, Q (Q in megawats).